We thank the reviewers and editors for their constructive comments on our manuscript. The manuscript is revised thoroughly by considering all the comments. Our responses to every comment are listed below with blue.

Response to Anonymous Referee 1

Summary

This paper presents an analysis of the peak altitude and peak emission rate of the hydroxyl (OH) emission rates observed for the past 20 years by the SABER instrument on the NASA TIMED satellite. SABER measures OH emission in two distinct spectral intervals, one centered at 2.0 um and the other at 1.6 um. The paper analyzes and presents results for the 1.6 um channel. The 20 years of SABER data enable comprehensive analysis of various temporal features that appear in the peak height and peak altitude of the OH emission. The analysis presented in the paper shows clear evidence for semi-annual and annual oscillations in the peak features and evidence for influence of the stratospheric quasi-biennial oscillation on the peak features. The results presented often confirm the results of previous papers regarding the presence of temporal features in the OH emission. The paper is clearly written.

The results in the paper are presented as 'engineering' analysis of the temporal variations in the OH emission. There is very little, if any, quantitative physics or chemistry given to explain the observed behavior. As an example, the discussion of solar variability is primarily of correlations between the OH variability and the F10.7 solar radio flux index. Solar variability affects temperature, composition, and dynamics. But the paper does not attempt to quantify which of these effects is dominant. The paper does not explain why there is strong latitude dependence in many of the analyses. However, the SABER dataset includes temperature, atomic oxygen, atomic hydrogen. These datasets could be explored along with model simulations (the WACCM model would be ideal for this) to put the results in context. In addition, although a secondary concern, the paper does not state why the peak altitude and peak emission rates are important physically. They are clearly markers for atmospheric variability. But is the variability important and why? One could imagine that since the reaction of H + O3 is the largest source of heating in the mesopause region, the variation in intensity and location of the OH emission means that the energetics of the mesopause are being altered significantly. Discussions such as this are necessary to place the results in a physical context as the reported variability largely reproduces prior works.

Recommendation

The recommendation is to reject the paper and invite submission of a new paper that contains much more detailed physical explanation of the observed OH behavior. This should include comparisons with the WACCM model and evaluations with other SABER data products. The paper should provide a quantitative explanation of features such as the latitudinal dependence of the semiannual and annual oscillations and should go into detail about the relative roles of temperature, chemistry, and dynamics in producing the observed variability.

We have completely revised the manuscript. The physical interpretation of the observed OH

emission variations is addressed in the responses to specific comments below. In addition, we have also used also the WACCCM model data and other SABER data products to provide a quantitative interpretation of features such as the latitudinal dependence of the semiannual and annual oscillations, and to detail the relative roles of temperature, chemistry, and dynamics in producing the observed variability.

A second recommendation is to evaluate the variability of the OH emissions on pressure surfaces and not on altitude. Studying variations at fixed altitudes mix variations in emission as the pressure surfaces rise and fall around the altitudes as the atmosphere warms and cools over the year and over the solar cycle. Pressure is the natural vertical coordinate of the SABER data.

While pressure is the natural vertical coordinate of the SABER data, the SABER data also provide altitude. One of the aspects we study is the variation in OH emission heights, and we do not study variations at a fixed altitude, but rather variable heights, both heights corresponding to peak emission rate and centroid altitude. The centroid altitude, i.e. altitude weighted by the emission rate profile.

Specific Comments

Title – the title contains the word 'trend' in relation to the peak OH emission. The word 'trend' typically implies looking at the long-term change of a parameter due to some forcing that is fundamentally changing the atmosphere such as increasing carbon dioxide concentrations. The original time series is analyzed in a way to remove variability (such as the AO, SAO, QBO, and solar cycle) and the linear trend of the residual is computed to derive a change (typically parameter per decade units). The paper does not appear to contain a trend analysis of this type. Please correct the title and the few places in the text where the word 'trend' occurs

We have changed the title to SAO, AO, QBO, and Long-term variation of the OH airglow emission. The word "trend" has also been corrected where it appears in the text.

Data use – An error was discovered in the SABER data for dates after December 16, 2019. A new version, v2.08 is available for data after that date. Please visit the SABER data web site to review and please discard all v2.0 data after Dec 16 2019.

We discard all v2.0 data from 15 December 2019 onwards. Data from 15 December 2019 to 31 December 2022 use the new version v2.08.

Line 23-24. This sentence is an example of the lack of quantitative understanding of the airglow that comes across in the paper. The airglow intensity is not directly related to density and only indirectly related to temperature through the temperature dependence of the rate coefficient for the reaction of H and O3. The entire Introduction is full of generalities that makes one question whether the paper truly understands the physics of airglow generation including how and why it varies. A revised Introduction should directly address the physics/chemistry of OH formation and how it may vary, thus setting up the results and analysis with a model such as WACCM later in the paper.

The energy required for the airglow emission is supplied by solar electromagnetic radiation.

Through direct and indirect action, solar radiation excites atoms, molecules and ions in the upper atmosphere to higher energy states, and activates particles to emit photons when they transition from high energy states to lower energy states, i.e., generating airglow. The hydroxyl (OH) vibration-rotational band is generated by the radiation transition between the vibrational energy levels of the ground state of the OH electron. The source of its production mainly comes from the chemical reaction between hydrogen atoms and ozone:

$$O_3 + H \xrightarrow{k1} OH(v \leq 9) + O_2$$
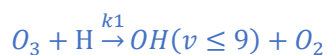
Line 116-117 – please provide a reference citation to the vibrational states that contribute to each of the SABER OH channels.

Russell, J., Mlynczak, M., Gordley, L., Tansock, J., and Esplin, R.: Overview of the SABER experiment and preliminary calibration results, SPIE's International Symposium on Optical Science, Engineering, and Instrumentation, SPIE1999. It's covered in this paper.

Line 125 – the instantaneous field of view of the SABER instrument is 2 km. SABER samples the atmosphere at a much higher cadence than every 2 km and so it may appear that the vertical resolution is much higher. The paper needs to discuss the effects of the finite field of view on the ability to determine and analyze variations of the peak height and emission.

The vertical resolution of the SABER observations is about 0.4 km, and the peak emission rate and peak height we obtained using a fit. The fitting corresponds to an altitude interval of 80-100 km, which has enough observation points to satisfy our need to determine and analyze the peak emission rate and peak altitude variations.

Line 136 – please provide a reference citation to the OMNI database and spell out the acronym.

For solar activity, we have used the solar irradiance representation measured by SEE (The Solar EUV Experiment). The F10.7 provided by OMNI, which was used previously, does not have the acronym found at URL https://omniweb.gsfc.nasa.gov/html/ow_data.html, where the data are provided.

Line 161, Section 3.1. The authors are encouraged to examine the data with Fourier techniques to see if other periodic features are evident.
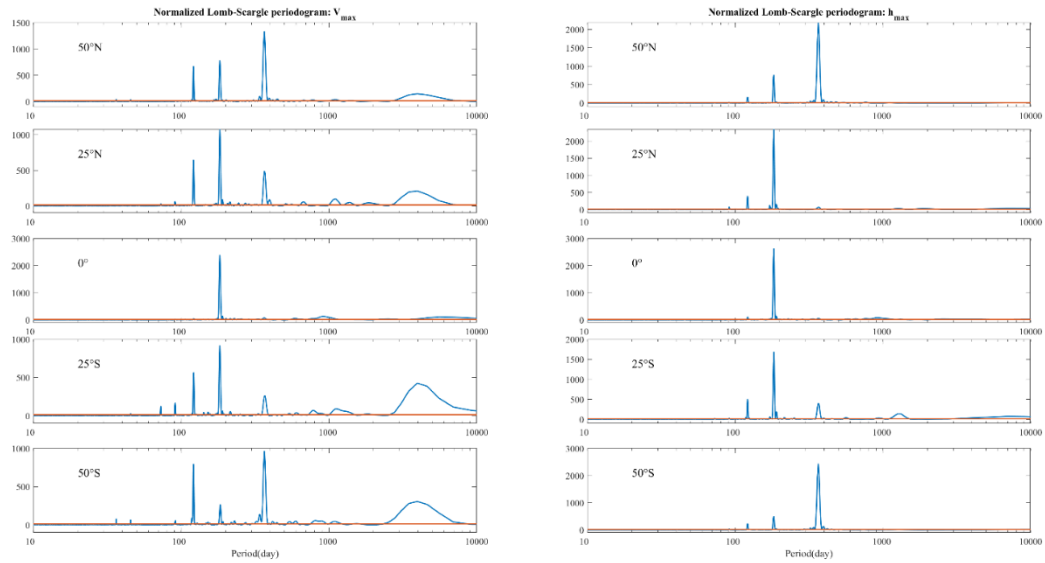
Figure 1: Lomb-Scargle periodograms calculated from V_{max}(left) and h_{max}(right) at five latitudes. The red lines denote the 99% confidence levels.

The periodograms of peak emission and peak height show that in addition to the 183-, 365-, 771- and 3965-day periodic features, there is also a 120-day periodic feature, which we have not analysed in this paper for the 120-day periodic feature.

Lines 181 to 200 – Any new manuscript should include explanations of the origins of the AO, SAO, and QBO, and how these influence the OH emissions. In particular, the AO should be primarily driven by the annual variation of earth-sun distance. So there is an annual cycle of solar radiation along with varying solar radiation on an 11 year cycle. Does any of the 11 year cycle 'alias' into the annual cycle? Could the Fourier techniques mentioned above help sort out different cyclic variations?

Theoretical studies generally agree that atomic oxygen between 80 and 100 km is controlled largely by downward transport from the thermosphere, where its abundances are very large and its photochemical destruction rate is slow(Garcia and Solomon, 1985). Huang and Hickey (2007) noted that vertical transport becomes important when species have long lifetimes and small scale heights. Since O has a relatively long chemical lifetime, O is mainly controlled by dynamics and less affected by chemistry. For species like O3 and OH*, which have smaller lifetimes, it is the combination of chemistry and dynamics that leads to much greater variability in these species.
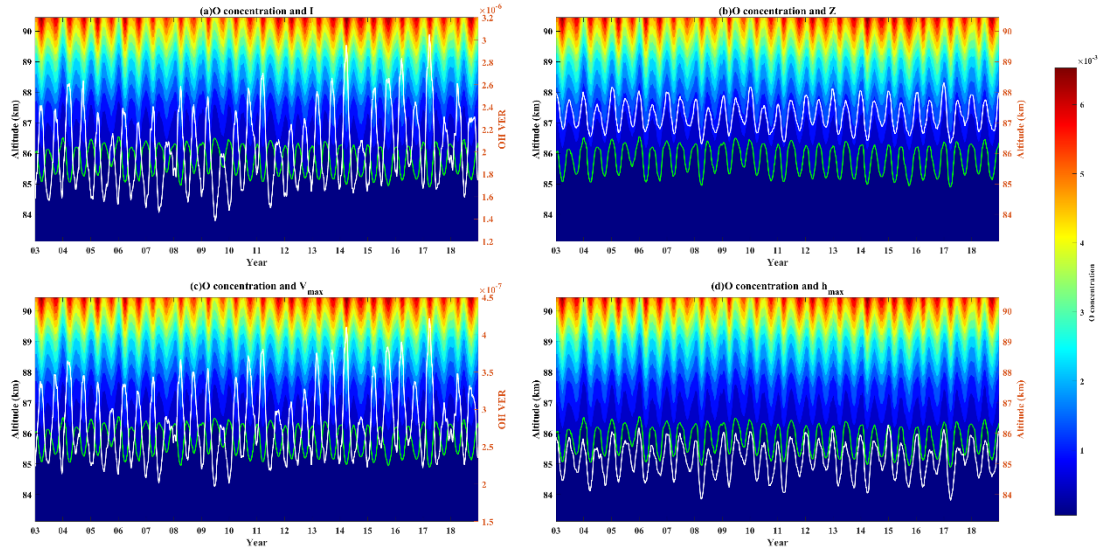
Figure 2: Contour plots of the zonal atomic oxygen concentrations in the equatorial (0°) zone predicted by SD-WACCM-X are shown. The green line refers to a contour line of O concentration. The white line is the parameter describing the OH airglow; the white line in Figure (a) is I, Z in Figure (b), V_{max} in Figure (c), and h_{max} in Figure (d).

Figure 2 shows the atomic oxygen concentration provided by the WACCM model. The green line in the figure represents a contour of the atomic oxygen concentration. We can find that the lower the height corresponding to the contour, the stronger the OH emission and the lower the emission height. The vertical transport of atomic oxygen shows a correlation with OH emission. As was noted above, a considerable amount of O is transported downwards，resulting in an increase in O at lower altitudes. Because of an increased downward flux of O, an increased amount of O is available to recombine with the major gases. Consequently, a large amount of O_3 is created through the three-body recombination reaction (reaction 2) due to the increased O, and then some of it destroyed in an exothermic reaction (reaction 1) to produce OH*. Since OH* is mainly produced through reaction 1, it is not surprising to find a large net increase in the OH* number density due to the increased loss of O_3 via reaction 1. The increase in OH* is a direct result of the increase in the amount of O3 reacting in reaction 1 and an indirect result of the increase in O transported vertically. By using a spectral full-wave dynamical model and a 2-D OH chemistry model, Huang and Hickey (2007) investigated the latitudinal variations of the wave effects on the minor species in the OH chemistry in the mesosphere/lower thermosphere region. They attributed the increase of the O number density at lower altitudes is due to wave transport, whereas the increase in the number densities of O_3 and OH* is due to the combination of wave transport and chemical effects with chemical effects dominating. They suggested that vertical wave transport of O coupling with chemistry could enhance the OH* volume emission rate because of a significant increase in the number density of the OH*. Therefore, vertical motion of O coupling with chemistry does seem to play a significant role in the enhancement of the OH* volume emission rate. They noted that the vertical motion of the species could be due to the action of gravity waves or to other types of waves, such as the tidal motion shown in Zhang and Shepherd (1999).
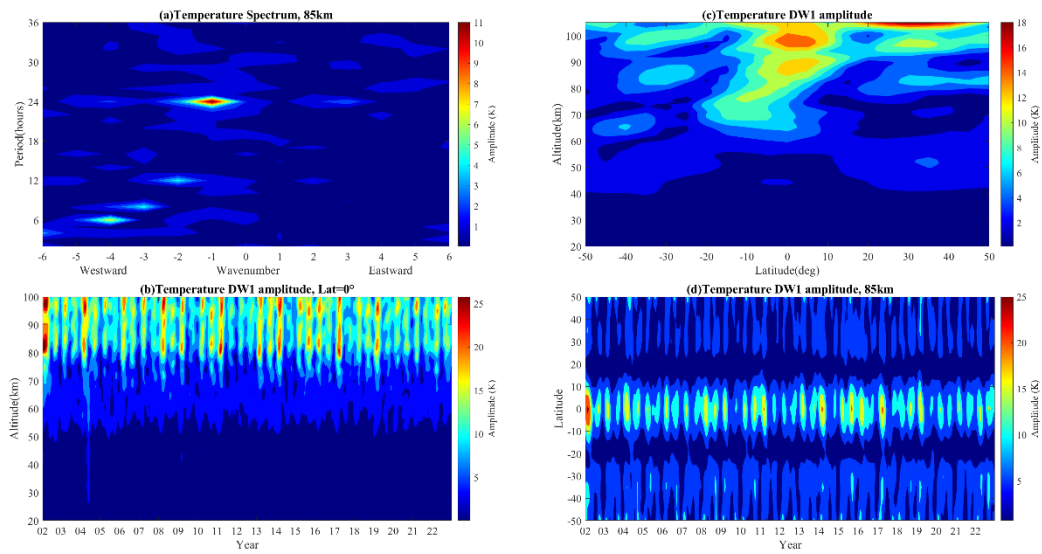
$$O_3 + \text{H} \xrightarrow{k1} OH(v \leq 9) + O_2 \tag{1}$$

$$O + O_2 + M \xrightarrow{k_{O+O_2+M}} O_3 + M \qquad\qquad (2)$$

Figure 3: (a)The wavenumber-period spectrum of SABER Temperature observations at 85 km and equator during day 152-212 of 2015. (b) The spatial structure of the DW1 amplitude on day 180 of 2015. (c) Temporal structure of the DW1 amplitude from 2003 to 2021. (d) Latitude-time distribution of the DW1 amplitude.

We calculated the amplitude of the 85 km diurnal tide using temperature data from SABER observations, choosing 85 km because the peak height is near 85 km. We analyse the tidal amplitude variations in correlation with the vertical transport of atomic oxygen, and there is SAO in both the tidal amplitude and the vertical transport of atomic oxygen, which may account for the presence of SAO in the OH emission.

Line 240-250 – please explain physically how the QBO in the stratosphere modulates the OH emission in the mesosphere.

QBO is present in both the tidal amplitude and the vertical transport of atomic oxygen, and stratospheric QBO affects the vertical transport of atomic oxygen in the same way that they affect the variation of the tidal amplitude. The increase in OH* is a direct result of the increase in the amount of O3 reacting in reaction 1 and an indirect result of the increase in O transported vertically.

Line 259-270. SABER has temperature, atomic oxygen, atomic hydrogen, and ozone data. These could be analyzed in concert with the OH data and WACCM model results to produce a complete picture of the relative importance of temperature, chemistry, and dynamics in producing the observed variations in the OH emission.
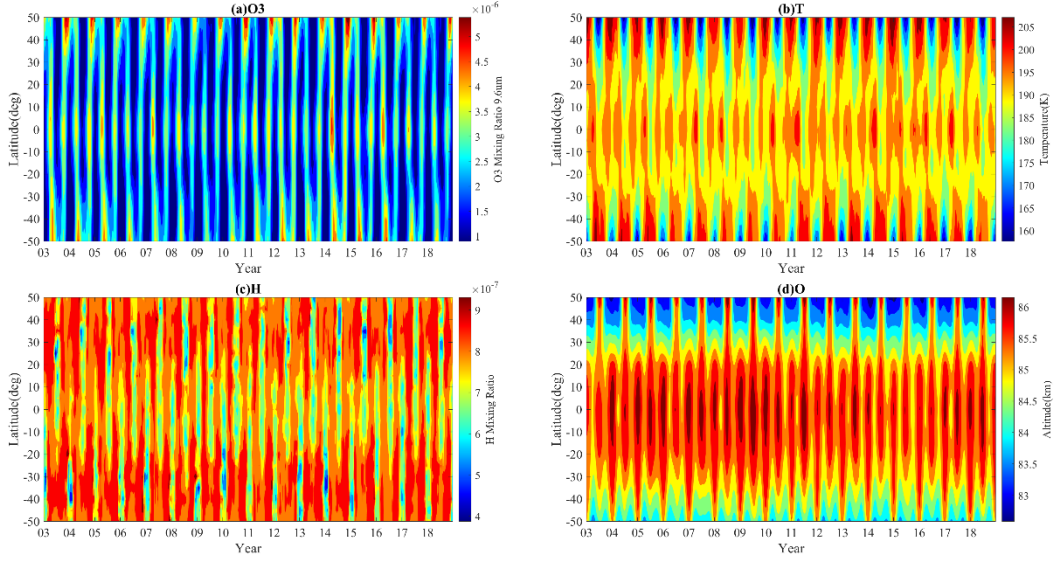
Figure 4: (a) Time-latitude distributions of ozone mixing ratio near 85 km. (b) Time-latitude distributions of temperature near 85 km. (c) Time-latitude distributions of H mixing ratio near 85 km. (d) Time-latitude distributions of heights corresponding to O concentration contours.

The ozone, temperature, and atomic hydrogen data from SABER were analyzed in concert with the atomic oxygen data from the WACCM model to provide a comprehensive understanding of the relative importance of temperature, chemistry, and dynamics in generating the observed variations in OH emission. We use a rather crude way of making comparisons by fitting the above quantities with the variation of the corresponding period such as SAO. The R2 statistic obtained from the fit indicates how well the relationship is explained. We believe that the more the variation of the corresponding period explains a quantity (the closer the R2 is to 1), the more that quantity plays a role in the appearance of that periodic variation in OH emission.

$$f = f_0 + a * \cos\left(\frac{2\pi}{183(day)}(t - t_{SAO})\right), \tag{3}$$

$$f = f_0 + a * \cos\left(\frac{2\pi}{365(day)}(t - t_{AO})\right), \tag{4}$$

As shown in Figure 4, (a), (b), and (c) demonstrate the time-latitude distributions of ozone, temperature, and atomic hydrogen near 85 km observed by SABER, respectively. (d) shows the height-time latitude distribution corresponding to the atomic oxygen concentration contour of the WACCM model. We fit the above quantities nonlinearly by least squares using the functions in Equation 3, respectively, and the fitted coefficients of determination (R-square) are shown in Figure 5(a).

We use O3 and H to denote chemical effects and the height of the O concentration contours to denote dynamic effects. As can be seen in Figure 5(a), the R^2 of both O3 and O in the equatorial region is very close to 1, which is consistent with our earlier interpretation that the vertical transport of atomic oxygen produces a large amount of O3 through Reaction 8, and then some of the O3 is destroyed in an exothermic reaction (Reaction 1) to produce OH*. The semi-annual oscillations of the OH airglow emission are the

result of the coupling of the vertical transport of atomic oxygen and chemical effects. Equation 4 was used to analyse the AO in the above quantities and the results are shown in Figure 5(b). Similar to OH emission, AO dominates near 50°N/S. In the results, the R^2 of the fitted temperature is close to 1, indicating that temperature is likely to be an important factor in the production of OH emission AO. In addition, Marsh et al. (2006) mention that AO in the higher latitude OH emission is consistent with transport by the downward component of the mean meridional circulation, which brings air rich in atomic oxygen from the lower thermosphere into the mesopause region.
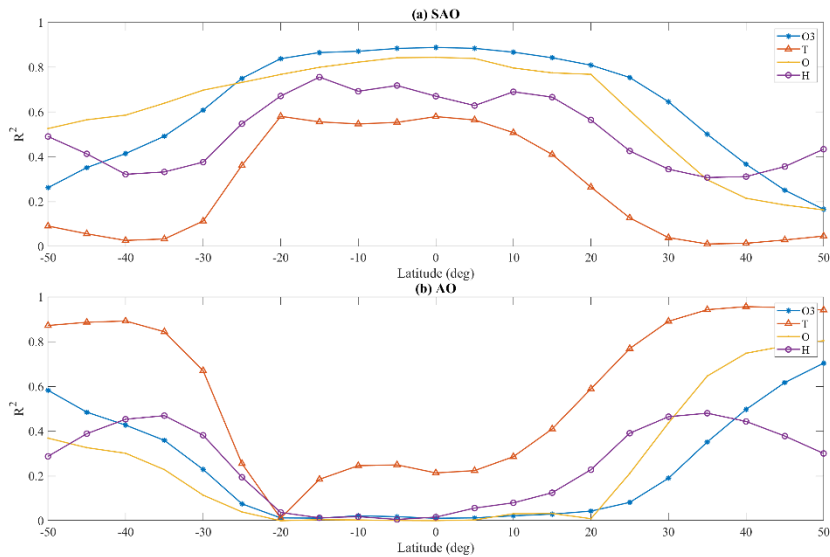

Figure 5: (a) The R^2 of the fitting results for each quantity in Figure10 using SAO. (b) The R^2 of the fitting results for each quantity in Figure10 using AO.

To facilitate the analysis of the relationship between OH airglow emission and stratospheric QBO, We choose a 365-day sliding temporal window with a step of 1 day to smooth OH emission rates and heights, which avoids the effect of seasonal variations on the analysis of the results. The smoothed results are shown in Figure 12, indicating the vertical integrated emission rate, centroid altitude, peak emission rate and peak height, respectively.
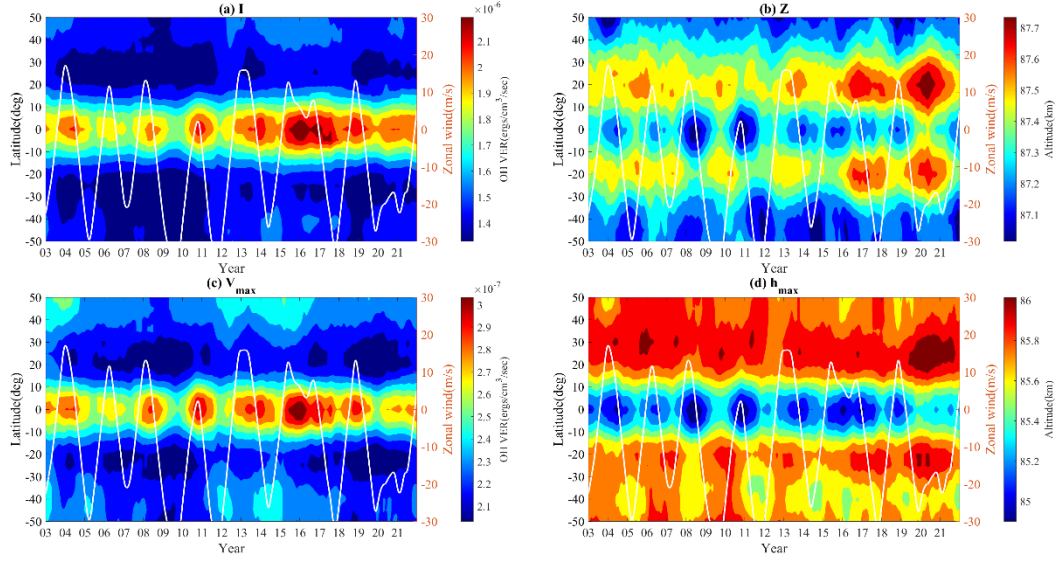
Figure 6: (a)Latitude-time distribution of the vertically integrated emission rate I. (b)Latitude-time distribution of the centroid altitude Z. (c)Latitude-time distribution of peak emission rate V_{max}. (d)Latitude-time distribution of peak height h_{max}. The white line refers to the daily average of the equatorial stratospheric zonal winds, smoothed like the four parameters of the OH airglow. A positive wind speed indicates an eastward wind.

In order to analyse whether the QBO signal in the OH emission is tidally correlated, we first smoothed the tidal amplitude in Figure 4(d) as in Figure 6, and the result is shown in Figure 7(a). The QBO signal is also shown in the diurnal tidal amplitude. Since QBO modulation of OH emission is also tidally correlated, whether it is observed in the vertical transport of atomic oxygen as in SAO is what we want to know. To explore the relative importance of temperature, chemistry, and dynamics on the QBO signal of OH emission, we performed the same smoothing with a window size of 365 days for the values in Fig. 10. A linear fit was then performed using Equation 5, and the R^2 of the fit is shown in Figure 7(b).

$$f = A + B * QBO \ , \tag{5}$$

where QBO represents the zonal wind data at 11 hPa in Singapore. At some latitudes, the R2 value when fitting H is larger than O. Xu et al. (2009) mentioned that SABER measured [O] and [H], but their errors are large, so we only use the SABER observation of [H] as a simple reference and not as the main analysis. In addition, at the equator, where the QBO signal is strongest, the R2 value is largest for O. The weak QBO signals for O3, H, and temperature suggest that dynamical processes play a more important role in producing the QBO signal for OH emission compared to temperature and chemical effects.
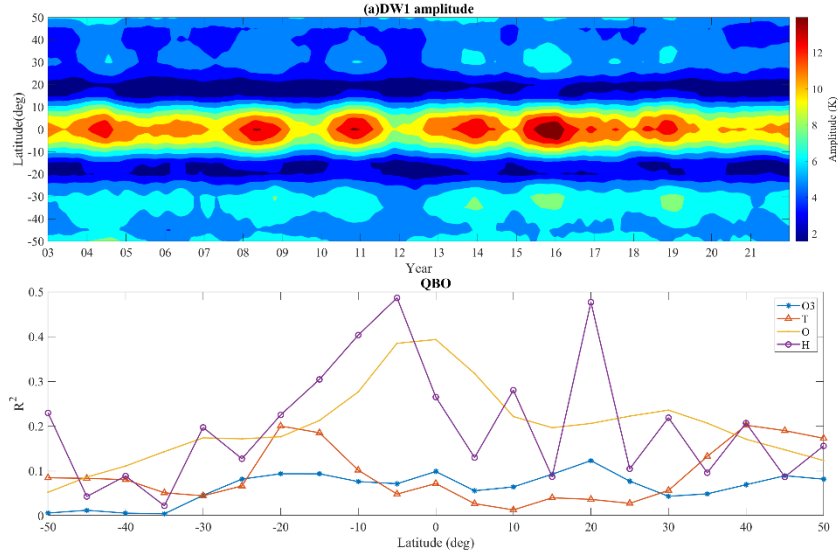
Figure 7: (a) Latitudinal-time distribution of the 85km diurnal tide amplitude. **(b)** O3, temperature, H and atomic contours of oxygen concentrations corresponding to heights associated with OH airglow emission. After fitting these quantities using the Singapore wind field, the R^2 statistics for different latitudes are shown in Fig.

Assuming that O3, temperature, H and O mentioned in Figure 10 are all linearly related to solar irradiance, we can use linear regression to calculate their response to solar activity and thus analyse which process dominates. A linear approximate regression model is used to describe the relationship between these quantities and solar irradiance:

$$f = A + B * Solar \ , \tag{12}$$

where Solar stands for solar irradiance.

Figure 8 shows the R^2 statistics for each latitude after fitting using solar irradiance. The comparison reveals that O3 has the largest R2 statistic, indicating that O3 (ozone-hydrogen reaction) has the largest relative role in the modulation of OH emission by solar activity. Tang et al. (2018) investigated the correlation between ozone concentration and solar activity using broadband emission radiometric atmospheric sounding (SABER) measurements and the 10.7-centimetre solar radiation flux (F10.7) dataset. He noted that O3 is determined by many factors under the radiative, chemical, and dynamical processes. With the increasing of UV irradiance, the solar activity index F10.7 increase, the production of ion pairs by photoionization (N2 and O2) and the production of atoms by O2 photodissociation increase, and thus, the abundance of O atoms vary with solar activity. The photochemical formation of ozone depends on solar activity. These may explain the reason that the interannual variation of O3 and [O] in mesopause are consistent with the 11-year solar cycle. The equatorial regions have R^2 statistics that are significantly smaller than those of other latitudinal regions, and those of the southern hemisphere are larger than those of the northern hemisphere. The response of OH airglow emission to solar activity shows the same pattern of latitudinal variation. The chemical reaction coefficient $k = 1.4 \times 10^{-10} \exp(-470/T) b(v)$ (Makhlouf et al., 1995) in reaction (1) where b(v) is positive. Temperature also has an effect on the emission of OH airglow. Marsh et al. (2006) compared SABER observations with a three-dimensional chemical transport model and found that most of the change in emissions was due to changes in ozone. Vertical transport of atomic oxygen is not the most important in the modulation

of OH emission by solar activity. However, the R^2 statistic at all latitudes is greater than 0.6, indicating that the vertical transport of atomic oxygen still plays an important role in the modulation of OH emission by solar activity. Therefore, we believe that chemical effects play the most important role in the modulation of OH emission by solar activity.
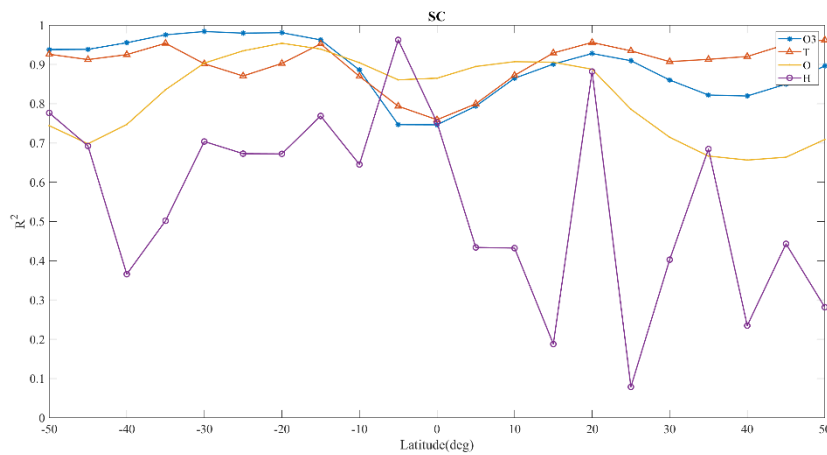

Figure 8: O3, temperature, H and atomic contours of oxygen concentrations corresponding to heights associated with OH airglow emission. After fitting these quantities using solar irradiance, the R^2 statistics for different latitudes are shown in Fig.

Line 300- Instead of using the F10.7 proxy, it is suggested to use the actual solar irradiance measured by the SORCE and SEE instruments over the past 20-plus years. Focus on the wavelength regions that drive most of the heating in the mesopause region. This may provide a much better result than using F10.7.

We have used solar irradiance to represent the intensity of solar activity, replacing the previous F10.7. The figure below shows the variation of the mean solar irradiance for wavelengths from 120.5 nm to 150.5 nm compared to the variation of F10.7. We chose a sliding time window of 365 days with a step size of 1 day to smooth the solar irradiance and F10.7.
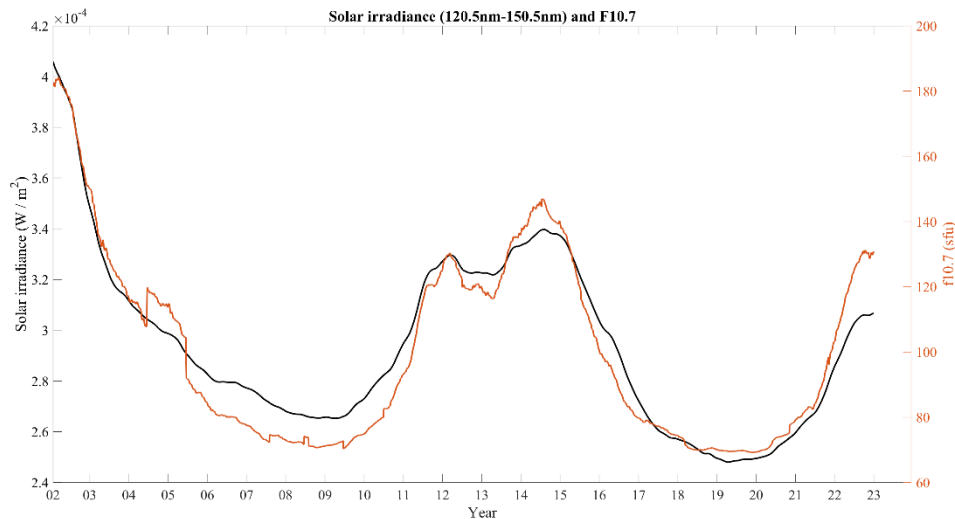
Figure 8: Solar irradiance vs. F10.7. The black line shows the change in mean solar irradiance from 120 nm to 150.5 nm and the red line shows the change in F10.7.

References

Garcia, R. R. and Solomon, S.: THE EFFECT OF BREAKING GRAVITY-WAVES ON THE DYNAMICS AND CHEMICAL-COMPOSITION OF THE MESOSPHERE AND LOWER THERMOSPHERE, J. Geophys. Res.-Atmos., 90, 3850-3868, 10.1029/JD090iD02p03850, 1985.

Huang, T. Y. and Hickey, M.: On the latitudinal variations of the non-periodic response of minor species induced by a dissipative gravity-wave packet in the MLT region, J. Atmos. Sol.-Terr. Phys., 69, 741-757, 10.1016/j.jastp.2007.01.011, 2007.

Makhlouf, U. B., Picard, R. H., and Winick, J. R.: PHOTOCHEMICAL-DYNAMICAL MODELING OF THE MEASURED RESPONSE OF AIRGLOW TO GRAVITY-WAVES .1. BASIC MODEL FOR OH AIRGLOW, J. Geophys. Res.-Atmos., 100, 11289-11311, 10.1029/94jd03327, 1995.

Marsh, D. R., Smith, A. K., Mlynczak, M. G., and Russell, J. M.: SABER observations of the OH Meinel airglow variability near the mesopause, J. Geophys. Res-Space Phys., 111, 14, 10.1029/2005ja011451, 2006.

Tang, C., Wu, B., Wei, Y., Qing, C., Dai, C., Li, J., and Wei, H.: The Responses of Ozone Density to Solar Activity in the Mesopause Region and the Mutual Relationship Based on SABER Measurements During 2002–2016, Journal of Geophysical Research: Space Physics, 123, 3039-3049, https://doi.org/10.1002/2017JA025126, 2018.

Xu, J., Smith, A. K., Liu, H.-L., Yuan, W., Wu, Q., Jiang, G., Mlynczak, M. G., Russell III, J. M., and Franke, S. J.: Seasonal and quasi-biennial variations in the migrating diurnal tide observed by Thermosphere, Ionosphere, Mesosphere, Energetics and Dynamics (TIMED), Journal of Geophysical Research: Atmospheres, 114, https://doi.org/10.1029/2008JD011298, 2009.

Zhang, S. P. P. and Shepherd, G. G.: The influence of the diurnal tide on the O(S-1) and OH emission rates observed by WINDII on UARS, Geophys. Res. Lett., 26, 529-532, 10.1029/1999gl900033, 1999.